

An Improved Control Strategy for a DC Gridbased Wind power Generation System in a Micro Grid

P.Sailaja¹ & G.Naresh² & G.Bhavanarayana³

¹PG Scholar, Dept. of EEE, Pragati Engineering College (A), E.G. District, AP, India.

² Professor, Dept. of EEE, Pragati EngineeringCollege (A),E.G. District, AP, India.

³Asst.Professor,Dept. of EEE, Pragati Engineering College (A), E.G. District, AP, India.

Received: May 29, 2018

Accepted: July 16, 2018

ABSTRACT

This paper presents an improved control strategy for a DC Grid based multiple parallel wind generation system by eliminating the need for voltage and frequency synchronization. Separate controllers are proposed for the inverter when grid is in grid-connected and islanded modes of operation. Model predictive control algorithm is used for the better transient performance with respect to the change in the operating condition for the inverter operation. Fuzzy logic controller is introduced for minimizing the fluctuations of the micro grid with the constant regulation of power. Aseparate controller has been developed for the wind turbine to maintain the constant power and to mitigate the variation error.Performance of the proposed micro grid in grid-connected and islanded modes is also evaluated.

Keywords: Wind power generation, Fuzzy controller, dc grid, energy management, model predictive control.

Introduction

According to the recent analysis of the Energy storage devices, and increase within the form of dc loads and therefore the penetration of dc distributed energy resources (DERs) like solar photovoltaic and fuel cells [1]. Several analysis works on dc micro grids are conducted to facilitate the combination of varied DERs and energy storage systems[2],[3]. A dc micro grid based mostly power station design during which every wind energy conversion unitconsistingof a matrix convertor, a high frequency electrical device and a single-phase ac/dc convertor is proposed[4]. However, the proposed design will increase the system quality as 3 stages of conversion are needed. In a dc micro grid based mostly power station design within which the WTs are clustered into teams of four with every cluster connected to a device is planned[5],[6]. However, with the proposed design, the failure of 1 device can lead to all four WTs of an equivalent group to be out of service[11],[12]. The analysis works conducted are focused on the event of various distributed management ways to coordinate the operation of varied DERs and energy[8],[10].

System Description

The general design of the proposed dc network based breeze control age framework for the poultry cultivate is appeared in Fig.1. The framework can work either associated with or islanded from the conveyance network and comprises of four 10 kW perpetual magnet synchronous generators (PMSGs) which are driven by the variable speed WTs. The PMSG is considered in this paper since it doesn't require a dc excitation framework that will expand the plan many-sided quality of the control equipment. The three-stage yield of each PMSG is associated with a three-stage converter (i.e., converters A, B, C and D), which works as a rectifier to control the dc yield voltage of each PMSG to the coveted level at the dc framework[10]. The total control at the dc matrix is reversed by two inverters (i.e., inverters 1 and 2) with each appraised at 40 kW. Rather than utilizing singular inverter at the yield of each wind generator (WG), the utilization of two inverters between the dc lattice and the air conditioner framework is proposed.

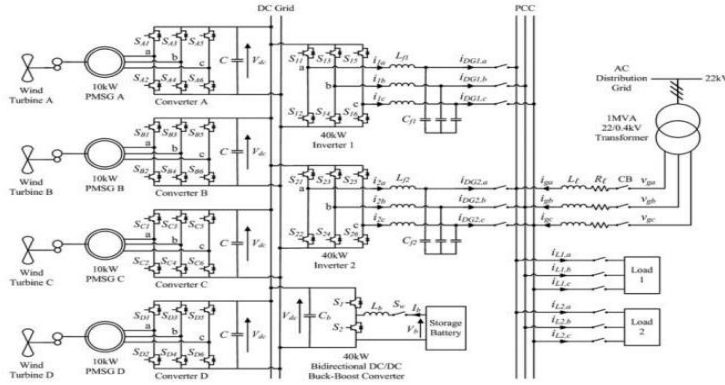


Fig.1. Overall configuration of the proposed dc grid based wind power generation system in a microgrid.

Instead of using individual inverter at the output of each WG, the use of two inverters between the dc grid and the ac grid is proposed[9]. This architecture minimizes the need to synchronize the frequency, voltage and phase, reduces the need for multiple inverters at the generation side, and provides the flexibility for the plug and play connection of WGs to the dc grid.

The centralized EMS is also responsible for other aspects of power management such as load forecasting, unit commitment, economic dispatch and optimum power flow[22],[23]. During normal operation, the two inverters will share the maximum output from the PMSGs. The maximum power generated by each WT is estimated from the optimal wind power as follows:

$$P_{wt,opt} = k_{opt}(\omega_{r,opt})^3 \tag{1}$$

$$k_{opt} = \frac{1}{2}C_{p,opt}\rho A \left(\frac{R}{\lambda_{opt}} \right)^3 \tag{2}$$

$$\omega_{r,opt} = \frac{\lambda_{opt}v}{R} \tag{3}$$

where k_{opt} is the optimized constant, $\omega_{r,opt}$ is the WT speed for optimum power generation, $C_{p,opt}$ is the optimum power coefficient of the turbine, ρ is the air density, A is the area swept by the rotor blades, λ_{opt} is the optimum tip speed ratio, v is the wind speed and R is the radius of the blade. The energy constraints of the SB in the proposed dc grid are determined based on the system-on-a-chip (SOC) limits given by

$$SOC_{min} < SOC \leq SOC_{max} \tag{4}$$

System Operation

When the micro grid is operating connected to the distribution grid, the WTs in the micro grid are responsible for providing local power support to the loads, thus reducing the burden of power delivered from the grid. The SB can supply for the deficit in real power to maintain the power balance of the micro grid as follows:

$$P_{wt} + P_{sb} = P_{loss} + P_l \tag{5}$$

Where P_{wt} is the real power generated by the WTs, P_{sb} is the real power supplied by SB which is subjected to the constraint of the SB maximum power $P_{sb,max}$ that can be delivered during discharging and is given

$$P_{sb} \leq P_{sb,max} \tag{6}$$

AC/DC Converter Modelling

Fig. 2 shows the power circuit consisting of a PMSG which is connected to an ac/dc voltage source converter. The PMSG is modeled as a balanced three-phase ac voltage source e_{sa},e_{sb},e_{sc} with series resistance R_s and inductance L_s . The state equations for the PMSG currents i_{sa},i_{sb},i_{sc} and the dc output voltage V_{dc} of the converter can be expressed as follows:

$$L_s \frac{di_s}{dt} = -R_s i_s + e_s - KSV_{dc} \tag{7}$$

$$C \frac{dV_{dc}}{dt} = i_s^T S - I_{dc} \tag{8}$$

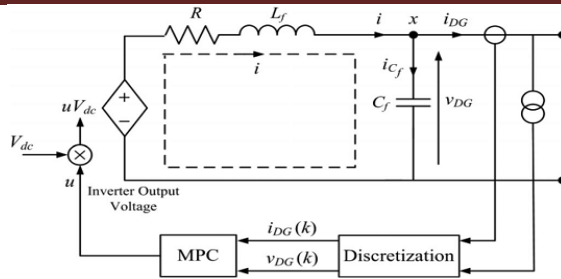


Fig. 2.Single-phase representation of the three-phase dc/ac inverter

DC/AC Inverter Modelling

The two 40 kW three-phase dc/ac inverters which connect the dc grid to the point of common coupling (PCC) are identical, and the single-phase representation of the three-phase dc/ac inverter is shown in Fig. 3.

To derive a state-space model for the inverter, Kirchhoff's voltage and current laws are applied to loop i and point x respectively, and the following equations are obtained:

$$S_j = \begin{cases} 1, & S_j \text{ is ON} \\ 0, & S_j \text{ is OFF} \end{cases} \quad \text{for } j = a, b, c \quad (9)$$

where Vdc is the dc grid voltage, u is the control signal, R is the inverter loss, Lf and Cf are the inductance and capacitance of the low-pass (LPF) filter respectively, iDG is the inverter output current, i is the current flowing through Lf, iCf is the current flowing through Cf, and vDG is the inverter output voltage.

During grid-connected operation, the inverters are connected to the distribution grid and are operated in the current control mode (CCM) because the magnitude and the frequency of the output voltage are tied to the grid voltage.

Thus, the discrete state-space equations for the inverter model operating in the CCM can be expressed with sampling time Ts as follows:

$$L_f \frac{di}{dt} + iR + v_{DG} = uV_{dc} \quad (10)$$

$$i_{DG} = i - i_{Cf} \quad (11)$$

The exogenous input vg(k) can be calculated using state estimation. In this paper, the grid is set as a large power system, which means that the grid voltage is a stable three-phase sinusoidal voltage. Hence, when operating in the CCM, a three-phase sinusoidal signal can be used directly as the exogenous input.

During islanded operation, the inverters will be operated in the voltage control mode (VCM). The voltage of the PCC will be maintained by the inverters when the microgrid is islanded from the grid. As compared to Ts, the rate of change of the inverter output current is much slower. Therefore, the following assumption is made when deriving the state-space equations for the inverter operating in the VCM [33]:

$$x_g(k + 1) = A_g x_g(k) + B_{g1} v_g(k) + B_{g2} u_g(k) \quad (12)$$

$$y_g(k) = C_g x_g(k) + D_g v_g(k) \quad (13)$$

Based on the above mentioned assumption, the discrete state space equations of the inverter model operating in the VCM can be expressed as follows

$$\frac{di_{DG}}{dt} = 0. \quad (14)$$

$$x_i(k + 1) = A_i x_i(k) + B_i u_i(k) \quad (15)$$

$$y_i(k) = C_i x_i(k) \quad (16)$$

During islanded operation, the inverters are required to deliver all the available power from the PMSGs to the loads. Therefore, only the inverter output voltage is controlled and the output current is determined from the amount of available power.

CONTROL DESIGN

Control Design for the AC/DC Converter

Fig. 4 shows the configuration of the proposed controller for each ac/dc voltage source converter which is employed to maintain the dc output voltage V_{dc} of each converter and compensate for any variation in V_{dc} due to any power imbalance in the dc grid [13],[14]. The power imbalance will induce a voltage error ($V_{dc}^* - V_{dc}$) at the dc grid, which is then fed into fuzzy controller to generate a current reference i_d^* for i_d to track.

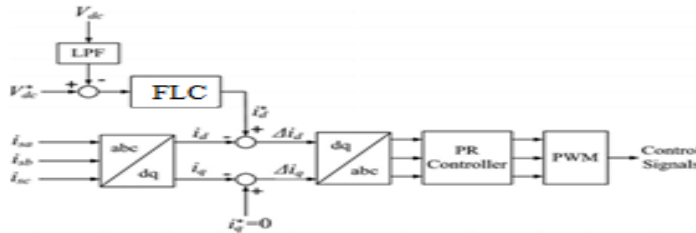


Fig. 3.Configuration of the proposed controller for the ac/dc converter.

Control Design for the DC/AC Inverter

In order for the microgrid to operate in both grid-connected and islanded modes of operation, a model-based controller using MPC is proposed for the control of the inverters. MPC is a model-based controller and adopts a receding horizon approach in which the optimization algorithm will compute a sequence of control actions to minimize the selected objectives for the whole control horizon, but only execute the first control action for the inverter [15],[16]. To derive the control algorithm for the inverters, the state-space equations are transformed into augmented state-space equations by defining the incremental variables in the following format:

$$\Delta\xi(k) = \xi(k) - \xi(k - 1) \tag{17}$$

where ξ represents each variable in the inverter model, such as v_{DG} , i_{DG} , i and u as shown in Fig. By defining the incremental variables, the augmented statespace model for the inverter model operating in the CCM during grid-connected operation can be expressed [17],[18] as follows:

$$X_g(k + 1) = A_{g_aug} X_g(k) + B_{g1_aug} V_g(k) + B_{g2_aug} U_g(k) \tag{18}$$

$$Y_g(k) = C_{g_aug} X_g(k) \tag{19}$$

Similarly, the augmented state-space model for the inverter model operating in the VCM during islanded operation can be expressed as follows:

$$X_i(k + 1) = A_{i_aug} X_i(k) + B_{i_aug} U_i(k) \tag{20}$$

$$Y_i(k) = C_{i_aug} X_i(k) \tag{21}$$

For the control of the two augmented models in the CCM and the VCM, the following cost function is solved using quadratic programming in the proposed MPC algorithm [33]:

$$J = (R_s - Y_j)^T (R_s - Y_j) + U_j^T Q U_j \tag{22}$$

Subject to the constraint

$$-1 \leq u_j(k) \leq 1 \tag{23}$$

III. FUZZY LOGIC CONTROLLER

In FLC, basic control action is determined by a set of linguistic rules. These rules are determined by the system. Since the numerical variables are converted into linguistic variables, mathematical modeling of the system is not required in FC

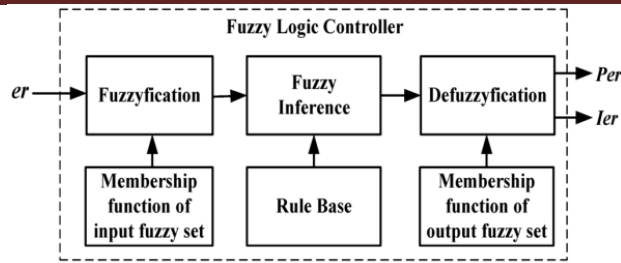


Fig.4.Fuzzy logic controller

The FLC comprises of three parts: fuzzification, interference engine and defuzzification. The FC is characterized as i. seven fuzzy sets for each input and output. ii. Triangular membership functions for simplicity. iii. Fuzzification using continuous universe of discourse. iv. Implication using Madman’s, ‘min’ operator. v. Defuzzification using the height method.

$$u = -[\alpha E + (1 - \alpha) * C] \quad [25]$$

Where α is self-adjustable factor which can regulate the whole operation. E is the error of the system, C is the change in error and u is the control variable.

SIMULATION RESULTS

The simulation model of the proposed dc grid based wind power generation system shown in Fig. 1 is implemented in MATLAB/Simulink. The system parameters are given in Table 1.

TABLE I: PARAMETERS OF THE PROPOSED SYSTEM

Parameter	Value
Distribution grid voltage	$v_g = 230 \text{ V (phase)}$
DC grid voltage	$V_{dc} = 500 \text{ V}$
PMSG stator impedance	$R_s = 0.2 \Omega, L_s = 2.4 \text{ mH}$
Distribution line impedance	$R_l = 7.5 \text{ m}\Omega, L_l = 25.7 \mu\text{H}$
Inverter LC filter	$L_f = 1.2 \text{ mH}, C_f = 20 \mu\text{F}$
Converter capacitor	$C = 300 \mu\text{F}$
Converter and inverter loss resistance	$R = 1 \text{ m}\Omega$
Load 1 rating	$P_{L1} = 35 \text{ kW}, Q_{L1} = 8 \text{ kVAr}$
Load 2 rating	$P_{L2} = 25 \text{ kW}, Q_{L2} = 4 \text{ kVAr}$

Test Case 1: Failure of One Inverter During Grid-Connected Operation

When the micro grid is operating in the grid-connected mode of operation, the proposed wind power generation system will supply power to meet part of the load demand. Under normal operating condition, the total power generated by the PMSGs at the dc grid is converted by inverters 1 and 2 which will share the total power supplied to the loads.

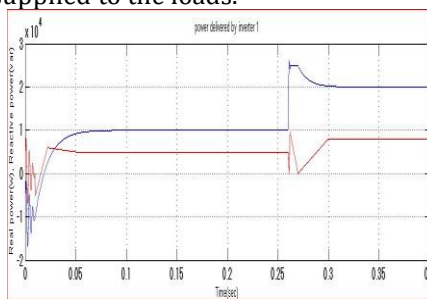


Fig. 1.1 Real (top) and reactive (base) control

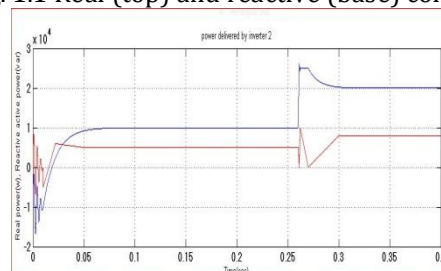


Fig. 1.2 Real (top) and reactive (base) control conveyed by inverter 1 conveyed by inverter 2

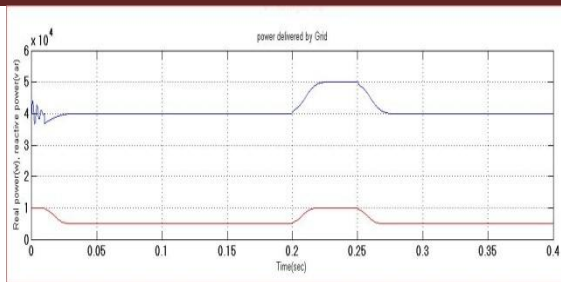


Fig. 1.3 Real (top) and reactive (base) control conveyed by the matrix
The total real and reactive power supplied to the loads is about 60 kW and 12 kVAR as shown in the power waveforms of Fig. 12.

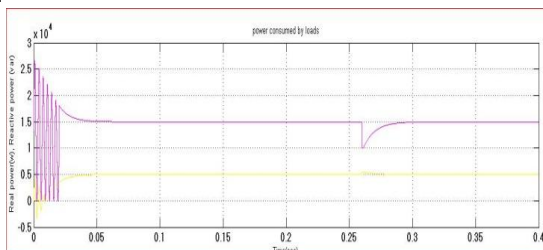


Fig. 1.4 Real (top) and reactive (bottom) power consumed by the loads.

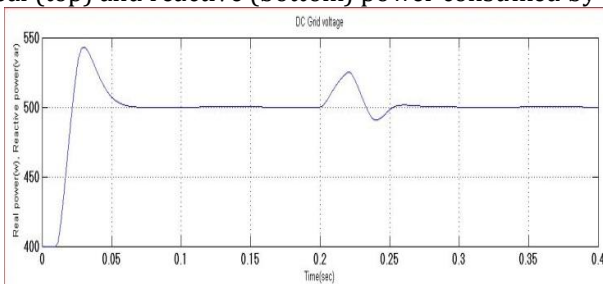


Fig. 1.5 DC Grid voltage.

This undelivered power causes a sudden power surge in the dc grid which corresponds to a voltage rise at $t = 0.2$ s as shown in Fig. 13.

Test Case 2: Connection of AC/DC Converter During Grid-Connected Operation

As shown in Figs. 14 and 15, each inverter delivers real and reactive power of 7 kW and 4 kVAR to the loads respectively

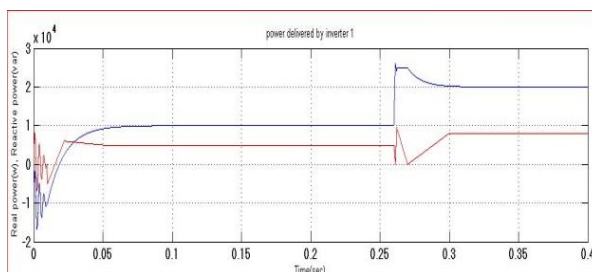


Fig. 2.1 Real (top) and reactive (base) control

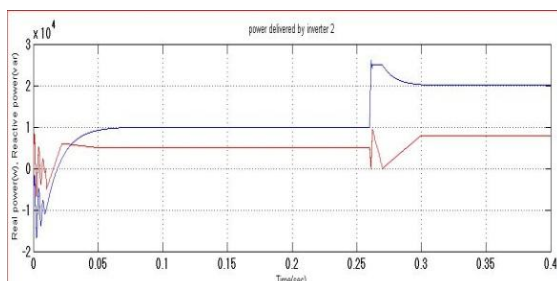


Fig. 2.2 Real (top) and reactive (base) control conveyed by inverter 1 conveyed by inverter 2.

The rest of the real and reactive power demand of the loads is supplied by the grid as shown in fig.

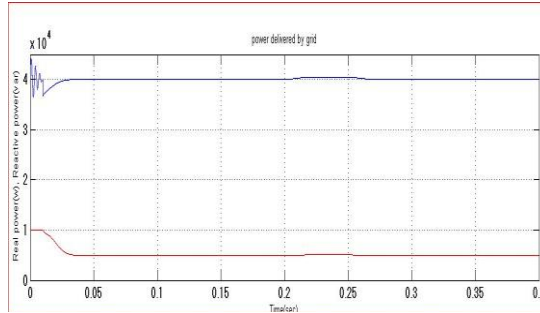


Fig. 2.3 Real (top) and reactive (base) control conveyed by the framework.

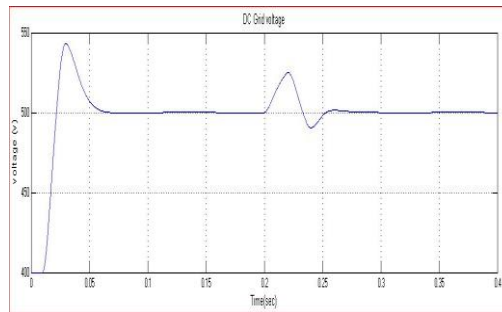


Fig 2.4 DC Grid voltage

It can be seen from Fig. 16 that the structure passes on 46 kW of honest to goodness power and 4 kVar of responsive vitality to the loads. This causes a promptly dunk in the dc grid voltage at $t = 0.26$ s as found in Fig. 17 which is then restored back to its apparent voltage of 500 V.

The matrix in the meantime lessens its supply to 40 kW of certifiable power for $0.26 \leq t < 0.4$ s while its responsive power remains predictable at 4 kVar as shown

C. Test Case 3: Islanded Operation

When the microgrid operates islanded from the distribution grid, the total generation from the PMSGs will be insufficient to supply for all the load demand. Under this condition, the SB is required to dispatch the necessary power to ensure that the microgrid continues to operate stably. The third case study shows the microgrid operation when it islands from the grid.

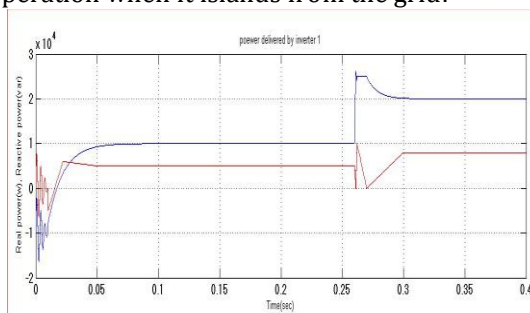


Fig.3.1 Real(top) and reactive (bottom) power delivered by inverter 1

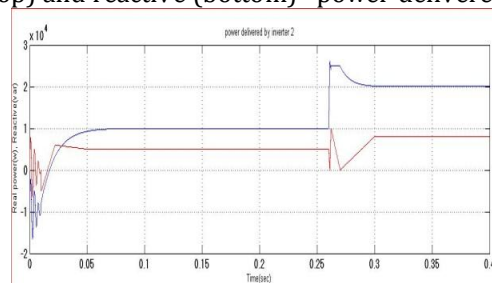


Fig.3.2 Real (top) and reactive (bottom) power delivered by inverter 2

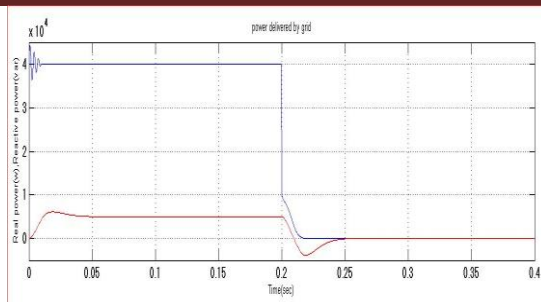


Fig .3.3 Real (top) and reactive (bottom) power delivered by grid.

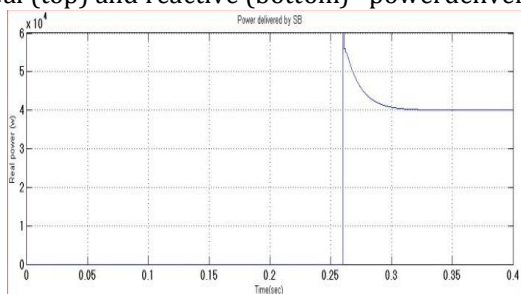


Fig 3.4 Real power delivered by SB.

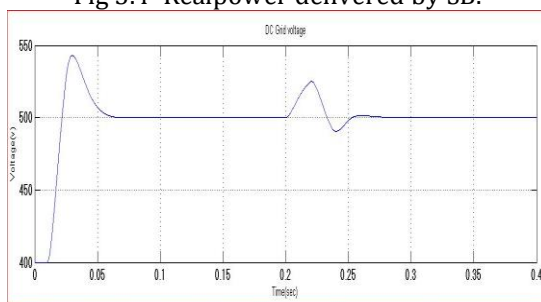


Fig 3.5 Real power delivered by Grid

CONCLUSION

This paper presents the operation of a dc grid-based wind power generation system that allows flexible operation of multiple parallel - connected wind generators by eliminating the need for voltage and frequency synchronization. By using a fuzzy logic based controller reduction of uncertain effects for better system control and improved efficiency are achieved. The design of a dc grid based wind power generation system in a microgrid enables parallel operation of several WGs has been presented in this paper. Compared to the conventional wind power generation systems, the proposed microgrid architecture eliminates the need for voltage and frequency synchronization, thus allowing the WGs to be switched on or off with minimal disturbances to the microgrid operation. In addition, Model predictive control proposed in this paper for controlling the inverters. A fuzzy based controller is introduced to increase the controller’s robustness against variations in the operating conditions.

REFERENCES

1. Farm Energy: Energy efficient fans for poultry production. [Online] Available: <http://farmenergy.exnet.iastate.edu>
2. A. Mogstad, M. Molinas, P. Olsen, and R. Nilsen, “A power conversion system for offshore wind parks,” in Proc. 34th IEEE Ind. Electron., 2008, pp. 2106–2112
3. A. Mogstad and M. Molinas, “Power collection and integration on the electric grid from offshore wind parks,” in Proc. Nordic Workshop Power Ind. Electron., 2008, pp. 1–8.
4. D. Jovic, “Offshore wind farm with a series multiterminal CSI HVDC,” *Elect. Power Syst. Res.*, vol. 78, no. 4, pp. 747–755, Apr. 2008.
5. M. Czarick and J. Worley, “Wind turbines and tunnel fans,” *Poultry Housing Tips*, vol. 22, no. 7, pp. 1–2, Jun. 2010.
6. The poultry guide: Environmentally control poultry farm ventilation systems for broiler, layer, breeders and top suppliers.

7. T. Dragicevi, J. M. Guerrero, and J. C. Vasquez, "A distributed control strategy for coordination of an autonomous LVDC microgrid based on power-line signaling," *IEEE Trans. Ind. Electron.*, vol. 61, no. 7, pp. 3313–3326, Jul. 2014.
8. N. L. Diaz, T. Dragicevi, J. C. Vasquez, and J. M. Guerrero, "Intelligent distributed generation and storage units for DC microgrids—A new concept on cooperative control without communications beyond droop control," *IEEE Trans. Smart Grid*, vol. 5, no. 5, pp. 2476–2485, Sep. 2014.
9. X. Liu, P. Wang, and P. C. Loh, "A hybrid AC/DC microgrid and its coordination control," *IEEE Trans. Smart Grid*, vol. 2, no. 2, pp. 278–286, Jun. 2011.
10. C. Jin, P. C. Loh, P. Wang, M. Yang, and F. Blaabjerg, "Autonomous operation of hybrid AC-DC microgrids," in *Proc. IEEE Int. Conf. Sustain. Energy Technol.*, 2010, pp. 1–7.
11. J. A. P. Lopes, C. L. Moreira, and A. G. Madureira, "Defining control strategies for microgrids islanded operation," *IEEE Trans. Power Syst.*, vol. 21, no. 2, pp. 916–924, May 2006.
12. Y. Li, D. M. Vilathgamuwa, and P. Loh, "Design, analysis, and real-time testing of a controller for multibus microgrid system," *IEEE Trans. Power Electron.*, vol. 19, no. 5, pp. 1195–1204, Sep. 2004.
13. C. L. Chen, Y. B. Wang, J. S. Lai, Y. S. Lai, and D. Martin, "Design of parallel inverters for smooth mode transfer of microgrid applications," *IEEE Trans. Ind. Electron.*, vol. 25, no. 1, pp. 6–15, Jan. 2010.
14. S. Kouro, P. Cortes, R. Vargas, U. Ammann, and J. Rodríguez, "Model predictive control—A simple and powerful method to control power converters," *IEEE Trans. Ind. Electron.*, vol. 56, no. 6, pp. 1826–1838, Jun. 2009.
15. K. S. Low and R. Cao, "Model predictive control of parallel-connected inverters for uninterruptible power supplies," *IEEE Trans. Ind. Electron.*, vol. 55, no. 8, pp. 2884–2893, Aug. 2008.
16. J. Rodríguez and P. Cortes, *Predictive Control Power Converters Electrical Drives*. Hoboken, NJ, USA: Wiley, 2012.
17. S. Mariethoz, A. Fuchs, and M. Morari, "A VSC-HVDC decentralized model predictive control scheme for fast power tracking," *IEEE Trans. Power Del.*, vol. 29, no. 1, pp. 462–471, Feb. 2014.
18. M. Korpas and A. Hølen, "Operation planning of hydrogen storage connected to wind power operating in a power market," *IEEE Trans. Energy Convers.*, vol. 21, no. 3, pp. 742–749, Sep. 2006.
19. M. Falahi, S. Lotfifard, M. Eshani, and K. Butler-Purry, "Dynamic model predictive-based energy management of DG integrated distribution systems," *IEEE Trans. Power Del.*, vol. 28, no. 4, pp. 2217–2227, Oct. 2013.
20. D. E. Olivares, A. Mehrizi-Sani, A. H. Etemadi, C. A. Canizares, R. Iravani et al., "Trends in microgrid control," *IEEE Trans. Smart Grid*, vol. 5, no. 4, pp. 1905–1919, Jul. 2014.
21. N. Mendis, K. M. Muttaqi, S. Sayeef, and S. Perera, "Standalone operation of wind turbine-based variable speed generators with maximum power extraction capability," *IEEE Trans. Energy Convers.*, vol. 27, no. 4, pp. 822–834, Dec. 2012.